HHS Public Access

Author manuscript

J Biomed Sci Eng. Author manuscript; available in PMC 2018 November 05.

Published in final edited form as:

J Biomed Sci Eng. 2017 November ; 10(11): 550–561. doi:10.4236/jbise.2017.1011041.

Development of an Artificial Finger-Like Knee Loading Device to Promote Bone Health

Sandeep Korupolu[1], **Stanley Chien**[2], **Hiroki Yokota**[3], and **Sohel Anwar**[1]

[1]Department of Mechanical Engineering, Indiana University Purdue University Indianapolis (IUPUI), Indianapolis, IN, USA

[2]Department of Electrical and Computer Engineering, Indiana University Purdue University Indianapolis (IUPUI), Indianapolis, IN, USA

[3]Department of Biomedical Engineering, Indiana University Purdue University Indianapolis (IUPUI), Indianapolis, IN, USA

Abstract

This study presents the development of an innovative artificial finger-like device that provides position specific mechanical loads at the end of the long bone and induces mechanotransduction in bone. Bone cells such as osteoblasts are the mechanosensitive cells that regulate bone remodelling. When they receive gentle, periodic mechanical loads, new bone formation is promoted. The proposed device is an under-actuated multi-fingered artificial hand with 4 fingers, each having two phalanges. These fingers are connected by mechanical linkages and operated by a worm gearing mechanism. With the help of 3D printing technology, a prototype device was built mostly using plastic materials. The experimental validation results show that the device is capable of generating necessary forces at the desired frequencies, which are suitable for the stimulation of bone cells and the promotion of bone formation. It is recommended that the device be tested in a clinical study for confirming its safety and efficacy with patients.

Keywords

Osteoblasts; Mechanical Loading; Artificial Hand; Bone Growth

1. Introduction

Mechanical loading is one of the major factors that influence bone architecture, since bone mineral density is significantly regulated by physical activity. During physical activity, mechanical forces are exerted on the bones through ground reaction forces and contractile

Correspondence to: Sohel Anwar, soanwar@inpui.edu.

Author Contributions

S.A. and H.Y. conceived the initial design of the device; S.K. and S.A performed the detail design of the mechanical and control systems for the device; S.K. and S.C. contributed to the electronic circuit design and microprocessor integration and programming; S.K. performed the experiments; S.A. and H.Y. analyzed the test data; S.K. and S.A. wrote the paper.

Conflicts of Interest

The authors declare no conflict of interest.

activity of muscles [1]. Bone mass can be increased in the presence on mechanical loading and reduced in its absence. It is proposed [2] that low-magnitude, high frequency mechanical stimuli are effective in evoking new bone formation or osteogenesis. In other words, if a small magnitude of mechanical stimuli is applied at a high frequency, an osteogenic response can be stimulated via mechanotransduction in bone cells.

In this study, we aimed to develop a device that is capable of generating transverse (sidewise) forces and applying directly to the end of long bones such as the knee. The present study is focused on the mechanical analysis for validating functionality of the device. Biomedical evaluations should be performed in future clinical trials.

Osteocytes are the most abundant type of cells in bone tissue, and they constitute more than 90% of the cells in bone matrix. They are rooted in the calcified bone medium, and communicate with each other and with bone-forming osteoblasts through slender processes and gap junctions [3]. Osteocytes are highly mechanosensitive. Haversian system or osteon, one of the key components of a porous bone matrix, encloses a blood vessel in its center and sets up the canals known as Haversian canals or Volkmann's canals. Osteogenesis is induced by the process of osteoinduction in which premature cells are recruited, stimulated and developed into pre-osteoblasts. Osteogenesis can also result from osteoconduction which is the passive process of bone growth on surfaces such as bone-implant surfaces [4].

When rapid mechanical loading is applied at the end of long bone (e.g., knee), it is proposed that the interstitial fluid present around the osteocytes in the lacuna-canalicular network induces a pressure gradient and elevates nutrient transport throughout the porous network. The added nutrients facilitates bone remodeling, which may shorten the healing time of bone fractures, increase bone mineral density, and prevent bone loss and damage in patients with osteoporosis and osteoarthritis, respectively [5 6].

Commercial devices such as an ultrasonic vibrator Exogen (bioventus, NC, USA), and Physio-Stim Lite (Orthofix, TX, USA) are in market in the field of assistive promotion of bone formation. For example, Exogen is wrapped around the leg, and generates ultrasonic waves for inducing physical stimuli [7]. Physio-Stim produces low magnitude high frequency signals and induces an electric field in bone tissue [8]. Several other devices are also available for inducing physical stimuli to bone [9 10]. To our knowledge, however, no devices are procurable that directly apply mechanical loading to the articular joint of long bones.

It is expected that transverse forces applied repetitively to the knee (distal femur) would transport the interstitial fluid towards the hip (proximal femur) in a controlled fashion. Although no clinical data are available, animal studies have been performed and effectiveness of this new type of loading is reported [11 14].

For testing knee loading, animal experiments were performed mainly on rodents and pigs. In one mouse experiment, surgical holes were drilled in their femurs on the middle part of the femur. A controlled mechanical loading was then applied on a periodic basis. It was observed that the surgical holes healed quickly in the femur with mechanical loading than the contralateral femur without mechanical loading [15]. This observation supports the

notion that direct mechanical loading is an effective treatment to accelerate healing of bone injuries. It also indicates that mechanical loading can potentially help in promoting bone health and can be used on humans as a preventive procedure to reduce a risk of hip fracture as well as a therapeutic procedure to enhance the healing of bone fractures. Based on the experimental studies, it was predicted that a maximum force of 40N with a frequency in the range of 1 to 5 Hz may maximize beneficial effects for loading on human knees [16]. It is recommended that the most appropriate loading condition (e.g., force magnitude and frequency) should be determined in a future clinical trial [17].

Based on the above loading estimates, an experimental mechanical loading device was initially developed that was able to apply varying magnitudes and frequencies of forces to the knee. The device incorporated a mechanism to apply distributed loading around the knee and was driven by a voice coil linear actuator (Figure 1) [16].

However, the preclinical studies indicated that the efficacy of inducing mechanotransduction of osteocytes depended on the stress distribution on the knee [11]. The knee is a complex structure anatomically as well as geometrically. Based on this observation, it is predicted that a position specific loading that provides a more targeted force application on the knee is likely to further improve induction of mechanotransduction [17].

2. Development of Multi-Fingered Artificial Hand

Many advanced robotic hands such as a “robotiq” robotic hand [18], a shadow robotic hand [19], Hiro-4 [20], SANDIA [21] etc. are available in the market, but they lack the capability to provide cyclic gentle loading. In order to provide a continuous position specific cyclic loading, this study was conducted for the development of the proposed artificial finger-like device, which is unique and first of its kind.

A mechanism is considered to be “under-actuated” if the number of actuators is a fewer than its degree of freedom. In the under-actuated mechanism, the motion is transmitted through mechanical linkages and elastic elements such as springs to actuate the passive joints. In the under-actuated finger, the actuation is applied to the bottom phalanges and is transmitted to other phalanges through mechanical elements such as pulleys and gears. In this study, the designed multi-fingered artificial hand is made up of 4 fingers with two phalanges, each connected by a torsion spring having 2 degrees of freedom.

The device should be able to apply necessary forces at required positions without generating any altering effects at any other locations. The device should be light in weight and should be capable to incorporate knees of various shapes and sizes.

For the safety of the patients, the design is subject to various constraints. The device should be compact, mobile, portable and run at low voltages, preferably less than 25 V. The device should be lightweight and preferably weigh less 4 kg. The device should produce a wide range of forces with a maximum force magnitude of 20N on each side and should run at various frequencies with a maximum frequency of 5 Hz.

2.1. Design Process

Four fingers having two phalanges each are designed. The two phalanges are connected by a revolute joint and a torsion spring is placed at the joint. A compliant soft plastic or rubber material is used to cover the distal phalange. The reaction force generated at the knee is proportional to the torsion spring displacement. Figure 2 represents the CAD drawing of the device.

Each finger is designed to produce a maximum force of 20N so that a set of fingers can produce 40N of force. The torsion spring prevents the additional displacement that limits the maximum force applied. Thus, it acts as a safety feature and provides a cushion to the knee. Figures 3(a)-(c) represent the motions of the finger in one cycle. Finger is connected to the finger base by a revolute joint and angularly oscillates on that revolute axis.

The stroke length of the slider dictates the displacement of the finger. Various slots are made on the crank wheel in the actuation mechanism to connect the slider. Thus changing the stroke length which limits the finger displacement and the maximum force applied. Figure 3(d) represents the variable displacement CAD model.

Each pair of fingers are connected and operated by slider and crank mechanism. A worm gear mechanism is used to transmit the motion from the actuator to the two sets of slider crank mechanism.

Basing on the FEA analysis results in [17], fingers and the base are 3D printed with ABS plastic material while aluminum and steel are considered for remaining components of the device.

2.2. Dynamic Formulation of the Finger

A dynamic analysis of the finger mechanism was performed using the Euler-Lagrangian method in [16]. The dynamic equations for the finger mechanism are given by:

$$T_1 = \left\lfloor I_1 + m_1 d_1^2 + m_2 L_1^2 \right\rfloor \ddot{p}_1 + \left\lfloor L_1 d_2 + L_1 L_2 \right\rfloor \ddot{p}_2 \cos(p_1 - p_2) - \left\lfloor L_2 d_2 + L_1 L_2 \right\rfloor (\dot{p}_1 - \dot{p}_2 \quad (1)$$
$$)p_2 \sin(\dot{p}_1 - \dot{p}_2) + \left\lfloor m_2 d_2 + L_2 \right\rfloor L_1 \dot{p}_1 \dot{p}_2 \sin(p_1 - p_2) + \left\lfloor m_1 d_1 + m_2 L_1 \right\rfloor g \cos(p_1)$$

$$T_2 = \left\lfloor I_2 + m_2 d_2^2 + m_2 L_2^2 \right\rfloor \ddot{p}_2 + \left\lfloor m_2 d_2 + m_3 L_2 \right\rfloor L_1 \ddot{p}_1 \cos(p_1 - p_2) - \left\lfloor m_2 d_2 + m_3 L_2 \right\rfloor L_1 (\dot{p}_1$$
$$- \dot{p}_2) \dot{p}_1 \sin(p_1 - p_2) + k\dot{p}_2^2 + k\dot{p}_2 + \left\lfloor m_2 d_2 + m_3 L_2 \right\rfloor L_1 \dot{p}_1 \dot{p}_2 \sin(p_1 - p_2) + \left\lfloor m_2 d_2 \right\rfloor g \cos(p_2)$$
$$- k p_2 \dot{p}_2$$

(2)

where T_1 and T_2 are the generalized torques at joints J_1 and J_2, L_1 and L_2 are the lengths of the phalanges, d_1 and d_2 are the distances from center of the mass of the phalanges to the

respective joints, p_1 and p_2 are the respective angles made with the axis parallel to the base, k is the spring constant of torsion springs (Figure 4), I_1, I_2 are the moment of inertias and m_1 and m_2 are the masses of proximal and distal phalanges respectively.

2.3. Rigid Body Dynamics

Rigid body dynamic simulations were performed using Simmechanics module of Matlab-Simulink and the results are published in the reference article [17]. The CAD model from Creo was imported to SimMechanics toolbox in MATLAB. Components such as controller, spring load, etc. have been manually added to the SimMechanics model. The model was then simulated for various force magnitudes ranging from 1 to 20 N and oscillation frequencies ranging from 1 Hz to 5 Hz. The simulation results indicates that the device is capable of producing desired force magnitudes within the desired frequency ranges. Figure 5(a) and Figure 5(b) show the results from SimMechanics model simulation. More information on SimMechanics simulations of this device can be found in the reference article [17].

2.4. Finite Element Analysis of the Device Design

Static structural analysis and modal analysis have been performed using ANSYS workbench 15.0 and the results were published in [22]. The device was analyzed in two cases for deformed geometry, stress distribution and modal frequencies. In case 1, only metals were used [23], aluminum for fingers and base and steel for the actuation mechanism. The results shows that the stresses, deformations and modal frequencies were with in safe limits with a maximum stress of 11. 2 MPa resulting in a safety factor of 22.22 and a maximum deformation of 0.05 mm which is relatively very less with respective to the maximum displacement of the finger. The first modal frequency occurred at 102 Hz, which is much above the maximum operating frequency. Figure 6(a) and Figure 6(b) represent Von-Mises stresses and 1st mode deformation plot for case 1.

In case 2, ABS plastic [24] was used for fingers, base, and steel for the actuating mechanism. The results showed that maximum stress of 32.07 was generated with a safety factor of 7.81 and the first modal frequency occurred at 70 Hz, which was much higher than the operating frequency of the device. The maximum deformation was 1.5 mm, which was in acceptable limits. Figure 6(c) and Figure 6(d) represents the Von-Mises stresses and 1st mode deformation plot of case 2.

From the finite element analysis results of the device, it was evident that using ABS plastic for the fingers and body, steel for the actuating mechanism is a better solution, which greatly decreases the device weight, manufacturing costs, labor, etc.

2.5. Device Prototype and Experimental Setup

Utilizing the dynamic simulation results in [17] and finite element analysis results in [22], a prototype device was built using 3D-printing technology. The device is actuated with a brushless DC motor manufactured by Anaheim Automation (Anaheim, CA, USA) which is capable of running at 4000 RPM and can produce 1.6 N-m of torque. A worm drive gear mechanism manufactured by SDP/SI (New Hyde Park, NY, USA) is used to transmit the

power from motor to the fingers. Figure 7 shows the experimental setup for the device. The mannequin knee (brand: EZ-IO) was purchased online.

For optimal working of the device and safety of the human knee, measurement of the force and displacement is performed to ensure that the forces are within the set limits. Four contact based flexi force sensors from Tekscan (Tekscan, MA, USA) four flex angular displacement sensors from Mouser (Mouser electronics, CA, USA) have been used for force and displacement measurements. The user interface for the device (shown in Figure 8) was built in-house and consists of an LCD (Liquid Crystal Display), various circuit boards, and two knobs for selecting loading frequency as well as time duration of a loading session. Furthermore, it contains three buttons for power (black), start (yellow) and emergency stopping (red) the device. The operation frequency of the device can be controlled by using the speed controller in conjunction with the Arduino microcontroller (Adafruit Industries, New York City, NY, USA). The actuator (DC motor) speed is controlled by a digital potentiometer circuit that gets its inputs from the Arduino controller. This entire circuitry is enclosed in a 3D printed box that collectively forms the user interface.

For the safety and optimal performance of the device, a control system was designed based on force/ displacement feedback to ensure that the forces are within the set limits. Force and displacement are continuously measured during the operation of device. If the force magnitude is greater than the desired value, the position control system is activated which would command the motor to retract the fingers to their default open positions (Figure 8). An Arduino microcontroller is used to implement the control strategy.

Additionally, the torsion springs between the phalanges will accommodate extra displacement, which will further regulate the force acting on the knee.

2.6. Operational Procedure

The user interface will need to be switched on and the required settings must be dialed in. The required force can be set by adjusting the crank at required positions on the disc while the fingers are adjusted so that they are in contact with the knee. When the device is turned on and the loading cycle is started, the measured force and frequency are continuously monitored. If the force exceeds the desired magnitude, the safety control system is activated which first stops the motor and turns it in opposite direction to bring the fingers back to the default position.

While the actual force delivered to the bone is not the same as the force applied by the device, a portion of the applied for is transmitted to the bone. Additionally, the force transmitted to the bone has a direct correlation with the force applied by the device on the skin. This work focuses on the device force application capabilities while actual force-efficacy relationship will be established in a future clinical study.

3. Experimental Results & Discussion

The proposed knee loading device was tested at two different values of finger angular displacements: 40 degrees and 20 degrees and two values of force: 10N and 20N while the

frequencies of force application are set at 1 Hz, 3 Hz, and 5 Hz for each finger respectively. The spring constant for the torsion spring was 0.015 N-m/deg and the resulting force and displacement outputs as would be felt at knee model are plotted in the following figures. Figure 9(a) and Figure 9(b) represent the angular displacement of 20 degrees and force magnitude of 10N at 1 Hz frequency.

For the display of the results, an open source software called Megunolink was used by interfacing it with Arduino Uno controller. The software is used to convert the serial data from the sensors to waveforms for easier elucidation.

Figure 9(c) and Figure 9(d) represent the angular displacement of 40 degrees and force magnitude of 20N at 3 Hz frequency.

Due to the software limitations, the experimental readings for displacement and forces were taken independently and as a result, the displacement and force data shown in these figure are not synchronized.

Figure 9(e) shows the displacement variation with an amplitude of 40 degrees at an operating frequency of 5 Hz and Figure 9(f) represents the corresponding force variation with an amplitude of 20 N.

The rigid body dynamic simulation results from MATLAB sim mechanics are in accordance with the experimental results which in turn validates the simulation results. Initially the device was made with steel and aluminum. The components were machined using the conventional machines. With the help of finite element analysis, ABS plastic was found to be a suitable replacement for most of the device metal components. Thus the fingers and the base are replaced with ABS plastic. 3d printing technology was used in fabricating the components. Use of 3d printed plastic components resulted in significant reduction of the device weight. 3d printing technology gave us the flexibility to fabricate the exact geometry of the fingers and reduced the overall fabrication cost and time significantly when compared to the metal components.

It is observed from the experimental results that the prototype device is capable of producing a wide range of forces up to 20N at various operating frequencies ranging from 1 Hz to 5 Hz. From functionality and usability standpoint the device meets all the design requirements set forth.

4. Conclusion

A multi fingered under actuated artificial hand was developed with the aim of providing position specific joint loading to induce physical stimuli into bone cells. Rigid body dynamics and finite element analysis were performed to demonstrate the theoretical functionality of the device. The finite element simulations demonstrated that building a prototype model with ABS plastic and steel is feasible and economical. Utilizing those results, a prototype device was built using 3D printing technology, a DC motor, sensors, two embedded controllers, and an in-house built device user interface at Purdue School of Engineering and Technology, IUPUI. The device was mechanically tested for validating its

capability to generate various force magnitudes at desired frequencies. These results demonstrated that the device can generate wide range of forces at various frequencies (0 N - 40 N, 1 - 5 Hz). With this capability, this device can be replicated and made ready for a clinical trial for further efficacy evaluations.

5. FUTURE WORK

The Flexi sensors used in this device had low accuracy and reliability resulting in suboptimal dynamic performance of the closed loop control of the device. However, if these sensors can be replaced with load cells and angular displacement sensors at the specific joints in the future prototypes, such issues will be resolved.

The scope of this paper has been limited to validate the functionality of the device. i.e. whether the device can produce forces up to 20N/finger at frequencies up to 5 Hz. The device design can further be improved by selecting more sturdy and accurate force and displacement sensors, as well as improving other mechanical and control elements. The patient safety and efficacy evaluations will also need to be done in a future clinical study.

Acknowledgments

The research work presented in this paper was partially supported by a FORCES (Funding Opportunities for Research Commercialization and Economic Success) grant awarded by the Office of the Vice Chancellor for Research, Indiana University Purdue University Indianapolis and NIH R01AR52144.

References

1. Lanyon LE, et al. Bone Deformation Recorded in Vivo from Strain Gauges Attached to the Human Tibial Shaft. Acta Orthopaedica Scandinavica. 1975; 46:256–268. [PubMed: 1146518]
2. Ozcivici E, Luu YK, Rubin CT, Judex S. Low-Level Vibrations Retain Bone Marrow's Osteogenic Potential and Augment Recovery of Trabecular Bone during Reambulation. PLoS One. 2010; 5:e11178. [PubMed: 20567514]
3. Takano-Yamamoto T. Osteocyte Function under Compressive Mechanical Force. Japanese Dental Science Review. 2014; 50:29–39.
4. Albrektsson T, Johansson C. Osteoinduction, Osteoconduction and Osseointegration. European Spine Journal. 2001; 10:S96–S101. [PubMed: 11716023]
5. Lee C, Grad S, Wimmer M, Alini M. The Influence of Mechanical Stimuli on Articular Cartilage Tissue Engineering. Topics in Tissue Engineering. 2005; 2:1–32.
6. Health Quality Ontario. Pyrocarbon Finger Joint Implant: An Evidence-Based Analysis. Ontario Health Technology Assessment Series. 2004; 4:1–31.
7. Bioventus. Ultrasound Bone Healing System
8. Orthofix Inc. Physio-Stim. 2010
9. Anthem Inc.. Electrical Bone Growth Stimulation. Anthem Medicalpolicy; 2014. DME. 0000408/14/2014
10. Anthem Inc. Ultrasound Bone Growth Stimulation. Anthem Medical Policy; 2014. DME. 0000408/14/2014
11. Zhang P, Malacinski GM, Yokota H. Joint Loading Modality: It's Application to Bone Formation and Fracture Healing. British Journal of Sports Medicine. 2008; 42:556–560. [PubMed: 18048437]
12. Kwon RY, Meays DR, Tang WJ, Frangos JA. Microfluidic Enhancement of Intramedullary Pressure Increases Interstitial Fluid Flow and Inhibits Bone Loss in Hindlimb Suspended Mice. Journal of Bone and Mineral Research. 2010; 25:1798–1807. [PubMed: 20200992]

13. Zhang P, Su M, Liu Y, Hsu A, Yokota H. Knee Loading Dynamically Alters Intramedullary Pressure in Mouse Femora. Bone. 2007; 40:538–543. [PubMed: 17070127]
14. Zhang P, Turner CH, Yokota H. Joint Load-ing-Driven Bone Formation and Signaling Pathways Predicted from Genome-Wide Expression Profiles. Bone. 2009; 44:989–998. [PubMed: 19442616]
15. Zhang P, Yokota H. Knee Loading Stimulates Healing of Mouse Bone Wounds in a Femur Neck. Bone. 2011; 49:867–872. [PubMed: 21723427]
16. Fitzwater D, Dodge T, Chien S, Yokota H, Anwar S. Development of a Portable Knee Rehabilitation Device That Uses Mechanical Loading. Journal of Medical Devices. 2013; 7 Article ID: 041007.
17. Korupolu S, Anwar S, Yokota H, Chien S. ASME International Mechanical Engineering Congress and Exposition. Vol. 13. Houston: 2015. Development of an under Actuated Robotic Device for Knee Loading Applications; 19
18. Robotic. Robotic Hand. 2016
19. Shadow Robot Company. Shadow Dexterous Hand. 2016
20. Halabi O, Kawasaki H. Five Fingers Haptic Interface Robot HIRO: Design, Rendering, and Applications. In: Zadeh MH, editorAdvances in Hap-tics. InTech; 2010.
21. Sandia Corporation. Sandia Hand. 2016
22. Korupolu S, Anwar S, Yokota H, Chien S. Finite Element Analysis of an under Actuated Robotic Device for Knee Loading Applications. ASME International Mechanical Engineering Congress and Exposition. 2016
23. ANSYS Inc. Engineering Data. Release 15.0.
24. Stratasys ABS M30.

Figure 1.
Knee loading device with a voice coil linear actuator.

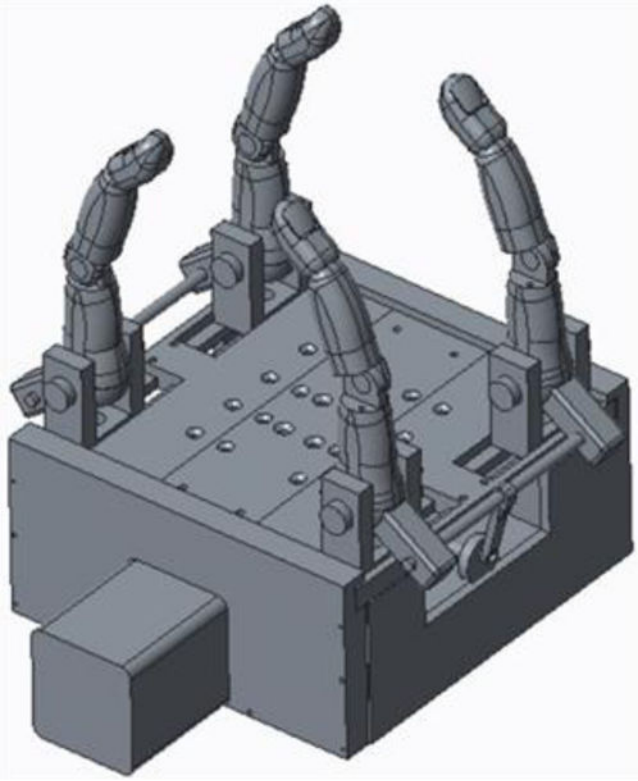

Figure 2.
CAD drawing of the proposed device.

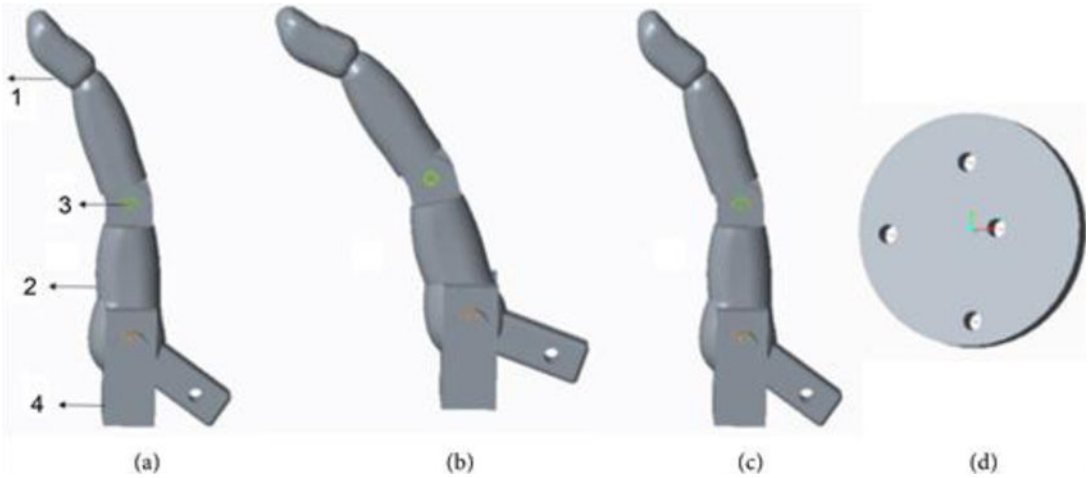

Figure 3.

(a)-(c) Motion of the finger in one cycle; (a) Initial position; (b) Load applying position; (c) final position; 1, 2: Phalanges, 3: Representation of a torsion spring, 4: Finger base; (d) variable displacement.

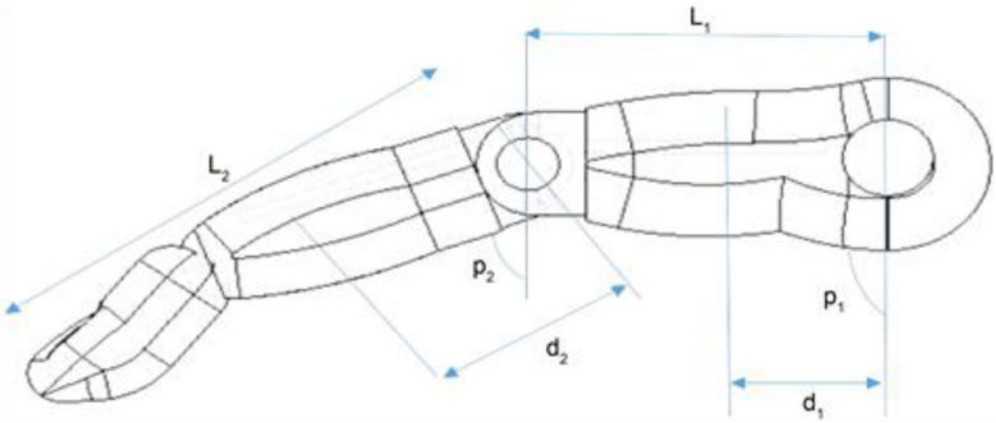

Figure 4.

Representation of a finger. L_1, L_2: Lengths of the Phalanges; d_1, d_2: Distances from center of the mass of the phalanges to the respective joints; p_1, p_2: Angles made with the axis parallel to the base.

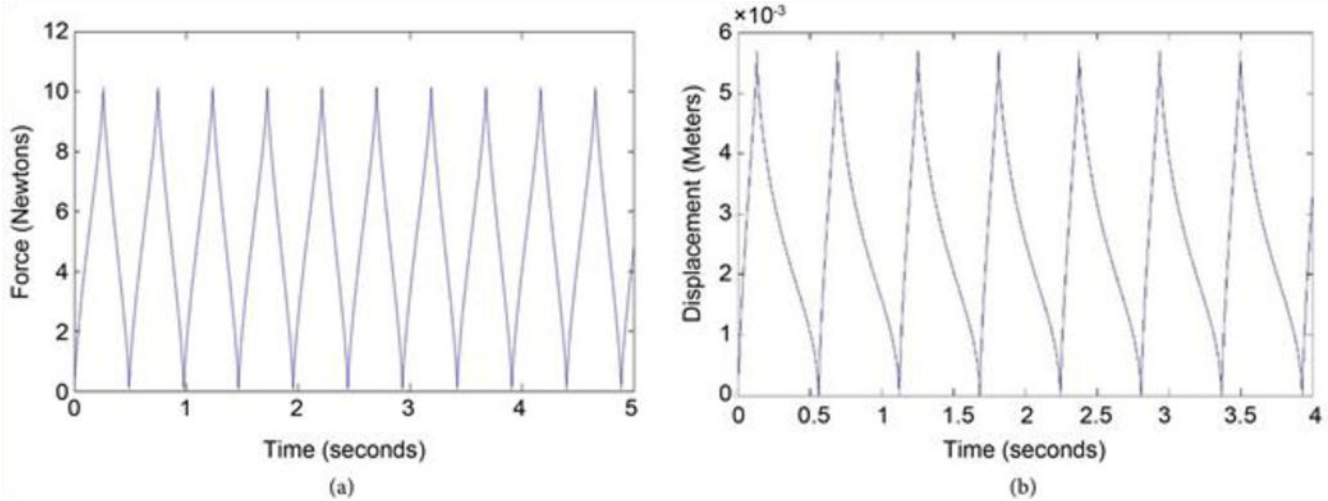

Figure 5.

Force responses. (a) Response to 10N at 2 Hz; (b) corresponding displacement response to 10N at 2 Hz.

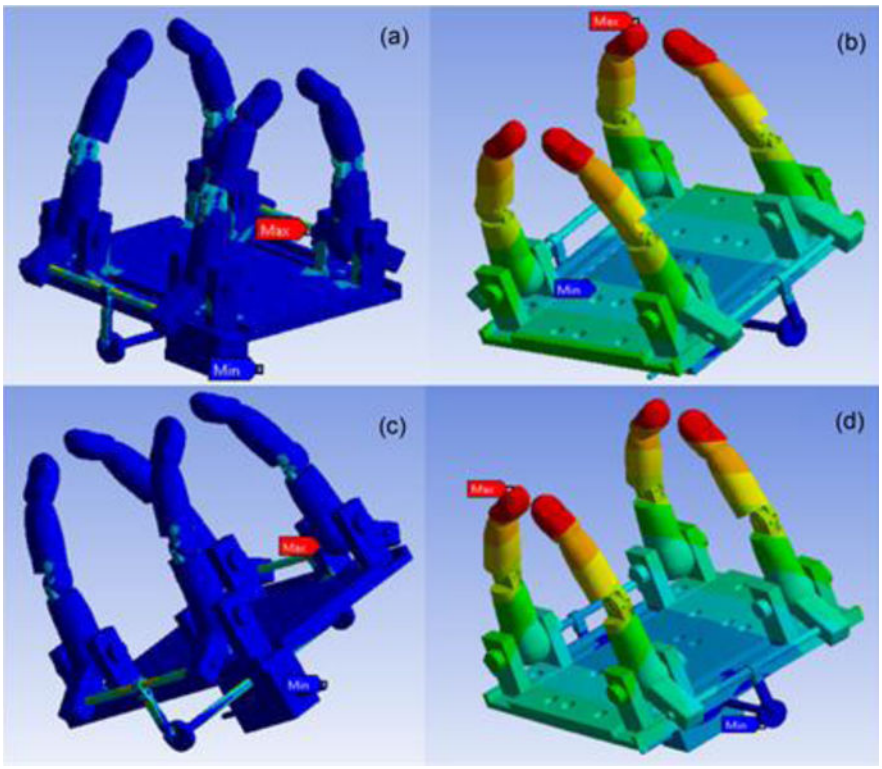

Figure 6.
(a) Case 1 Von Mises stress contour plot; (b) Case 1 Modal analysis results; (c) Case 2 Von Mises stress contour plot; (d) Case 2 modal analysis results.

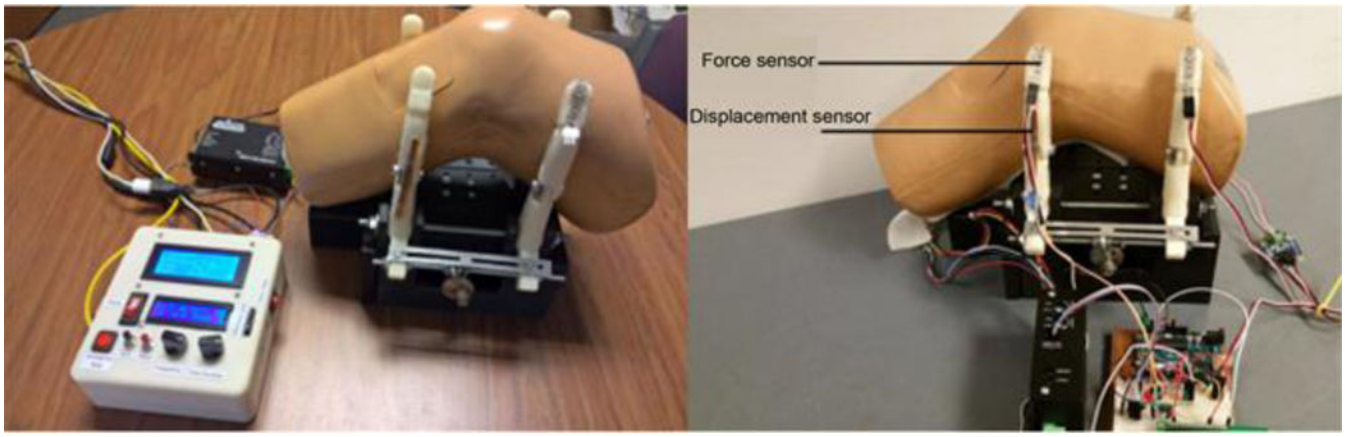

Figure 7.
Experimental setup of the device with artificial knee.

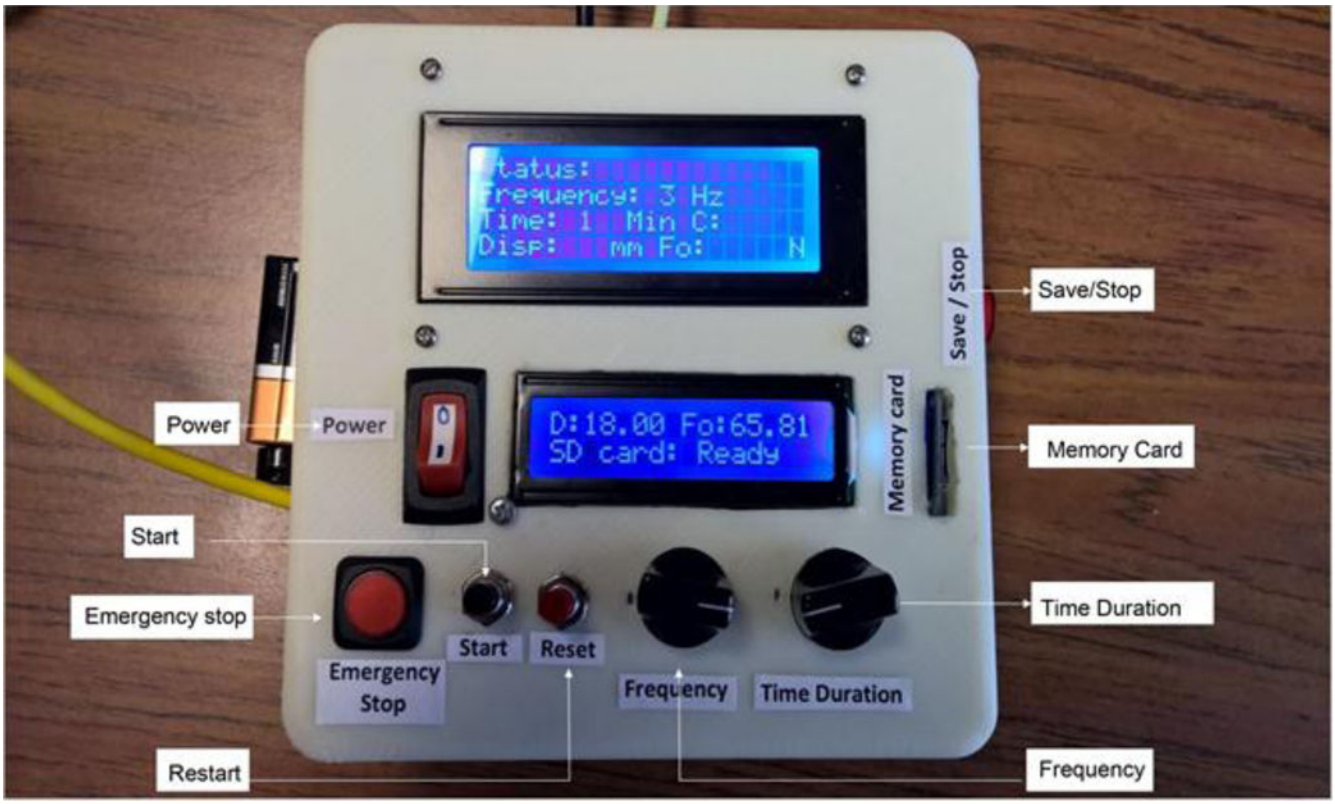

Figure 8.
Device user interface.

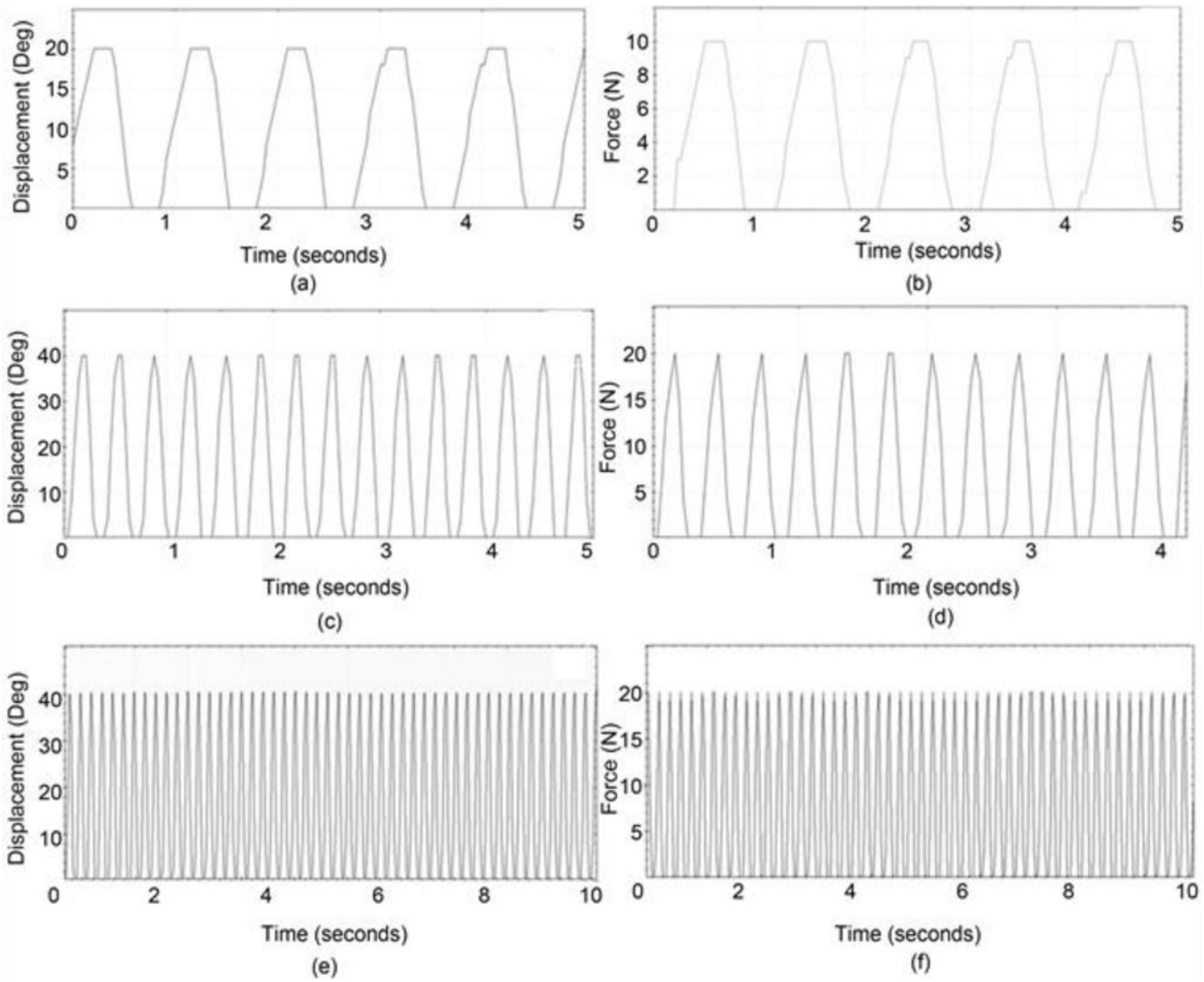

Figure 9.

Experimental results (a) Displacement of 20 degrees at 1 Hz; (b) force of 10N at 1 Hz; (c) displacement of 40 degrees at 3 Hz; (d) force of 20N at 3 Hz; (e) displacement of 40 degrees at 5 Hz; (f) force of 20N at 5 Hz.